

# Molecular Dissociation in Deuterium Sulfide under High Pressure: Infrared and Raman Study

Mami Sakashita,\* H. Fujihisa, H. Yamawaki, and K. Aoki

National Institute of Materials and Chemical Research, Tsukuba, Ibaraki 305-8565, Japan  
and CREST, Japan Science and Technology Corporation, Kawaguchi, Saitama 332-0012, Japan

Received: April 27, 2000; In Final Form: June 16, 2000

Experiments using a diamond-anvil cell show that deuterium sulfide ( $D_2S$ ) dissociates to form sulfur at pressures above 27 GPa and room temperature. Raman-scattering spectroscopy indicates the presence of S–S bonds of a high-pressure phase sulfur, helical sulfur, and eight-membered cyclic sulfur. On the other hand, infrared-absorption spectroscopy indicates the presence of S–D bonds of both polymeric and unreacted  $D_2S$ . The formation of sulfur from  $D_2S$  can be interpreted as reconstruction of chemical bonds at high pressures.

## Introduction

The high-pressure behavior of simple hydrogen-bonded molecular solids such as  $H_2O$ ,  $H_2S$ , and  $NH_3$  is of fundamental importance in understanding the nature of hydrogen bonds. Extensive studies of  $H_2O$  ice have explored changes in hydrogen bonds with pressure. Hydrogen sulfide ( $H_2S$ ) is a sister molecule of  $H_2O$ , but despite basically similar chemical compositions, they differ significantly in internal bond angle and strengths of hydrogen bonds. There has been considerable interest in knowing how these differences affect the high-pressure behavior.

$H_2S$  and  $H_2O$  show very different behavior in physical properties at high pressures or low temperatures. For example,  $H_2S$  has weaker hydrogen bonds than  $H_2O$ , so that  $H_2S$  molecules have a degree of rotational freedom in some crystal-line phases.<sup>1–3</sup> Another example is the color of  $H_2S$  and  $H_2O$  at high pressure. The transparent, colorless phase I' of  $H_2S$  becomes light yellow in phase IV above 11 GPa and subsequently black and opaque above 28 GPa.<sup>4</sup> These color changes suggest a large decrease in band-gap energy. On the other hand, all phases of  $H_2O$  studied up to 128 GPa are colorless and transparent.<sup>5</sup> No apparent change in the electronic state of  $H_2O$  has been reported.

The third example, molecular dissociation at high pressures, was identified by infrared-absorption or -reflection measurements for the proton-related vibrations. In the case of  $H_2S$ , while S–H stretching peaks soften only slightly, the disappearance of S–H stretching peaks and simultaneous appearance of a lattice vibrational peak near 46 GPa signal molecular dissociation.<sup>6</sup> At higher pressures, metalization seems to occur, as indicated by a low-energy electronic-absorption band that develops throughout the infrared region.<sup>6</sup> For  $H_2O$ , dissociation coincides with hydrogen-bond symmetrization: O–H stretching peaks soften remarkably under pressure as  $H_2O$  continuously changes from a molecular to an atomic solid in which the proton lies at the midpoint between two oxygens.<sup>7,8</sup>

Although the mechanism of molecular dissociation in  $H_2S$  is yet to be fully described, recent reports provide useful information. X-ray powder diffraction revealed that the structure of phase IV (11–28 GPa) is tetragonal  $D_{4h}^{20}-I4_1/acd$  and that its first nearest S–S distance is shorter than twice the van der Waals

radius of sulfur.<sup>3</sup> This suggests the possibility of the formation of S–S covalent bonds above 28 GPa, since the first nearest S–S distance is expected to become much shorter with increasing pressure. In addition, Raman studies of  $H_2S$  have found that lattice vibrational peaks change notably at the IV–V transition.<sup>9</sup> It is considered that molecular dissociation begins around 27–35 GPa on the basis of the Raman data. This dissociation pressure was about 15 GPa lower than that reported in infrared measurements.<sup>6</sup>

The purpose of the present work is to clarify the mechanism of molecular dissociation that occurred in  $H_2S$ . Our attention is mainly focused on the following three points: (1) what happens in the chemical bonds above 28 GPa; (2) whether S–S covalent bonds form above 28 GPa; (3) what initiates molecular dissociation. To answer these questions, we measured infrared and Raman spectra of solid deuterium sulfide ( $D_2S$ ) with a diamond-anvil cell. Raman measurement is helpful to confirm the formation of S–S bonds, since S–S stretching peaks are observed at frequencies lower than  $600\text{ cm}^{-1}$ . Whereas changes in the bonding state, occurring not only on the surface but also in the inner part of a sample, can be detected by infrared-absorption measurement. The  $D_2S$  sample enables us to assign vibrational peaks through the isotopic shift and to get further information about molecular dissociation. When hydrogen is replaced by deuterium, the frequencies of vibration are altered because of the large percentage change in mass. In addition, the transition pressures relating to hydrogen-bond symmetrization were found to be higher in  $D_2O$  by 10–15 GPa than in  $H_2O$ .<sup>7,8,10</sup>

## Experimental Section

Commercially obtained gaseous  $D_2S$  (97 at. % D) was used without further purification. A  $100\text{ }\mu\text{m}$  diameter and a  $50\text{ }\mu\text{m}$  thick sample chamber was drilled in a metal gasket (PK). The chamber was filled with solidified  $D_2S$ . Infrared-absorption spectra were measured with a microscope Fourier transform infrared spectrometer having a MCT detector. The spectral resolution was set to  $1\text{ cm}^{-1}$ , and each spectrum was accumulated 400 times. A reference spectrum of an empty diamond-anvil cell at atmospheric pressure was used to compensate for absorption by the diamond anvils. The 488 nm line of an argon ion laser was used for Raman excitation. Back-

\* TEL/FAX: +81-298-61-4426. E-mail: saka@home.nimc.go.jp.

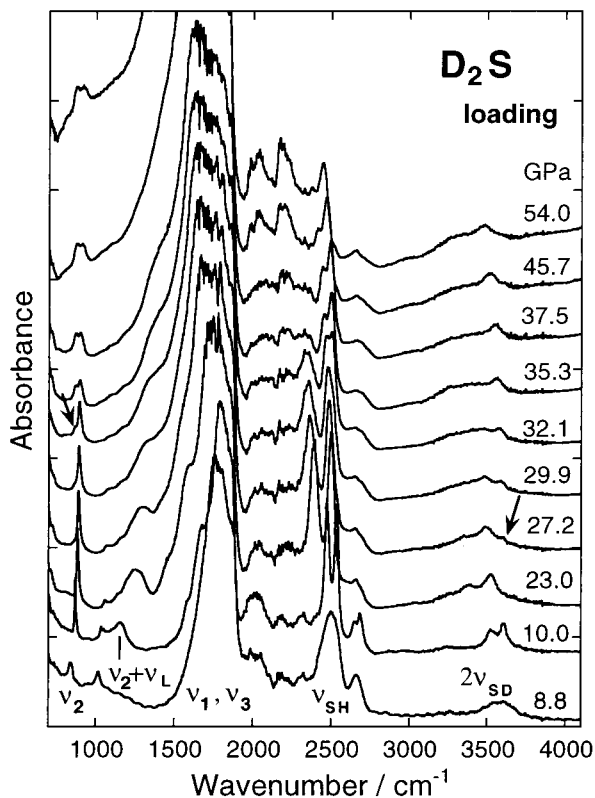


**Figure 1.** Infrared-absorption spectra of solid  $D_2S$  up to 54 GPa at room temperature. New infrared peaks marked with arrows appeared around 3580 and 870  $cm^{-1}$  above 27 GPa.

scattered light from the sample was analyzed using a single monochromator and two holographic notch filters. The filters were placed in front of the entrance slit of the monochromator to block the laser excitations. Raman spectra were recorded with a liquid nitrogen cooled CCD detector capable of covering a wavenumber region of 3000  $cm^{-1}$  at one time with a spectral resolution of 2.3  $cm^{-1}$ . The frequencies of Raman bands were calibrated both with spectral calibration lamps and with emission lines of the laser. Pressures were measured from shifts of the  $R_1$  fluorescence line from ruby chips embedded in the sample.<sup>11</sup>

## Results

Figure 1 shows changes in infrared-absorption spectra of  $D_2S$  measured up to 54 GPa. Deuterium substitution reduced the fundamental frequency by a factor of about  $1/\sqrt{2}$ . Broad peaks observed around 1700  $cm^{-1}$  were assigned to the fundamental S–D stretching modes ( $\nu_1$  and  $\nu_3$ ), and the peaks at 842 and 3590  $cm^{-1}$  at 8.8 GPa were assigned to a bending  $\nu_2$  and the overtone of the stretching modes ( $2\nu_{SD}$ ), respectively. Peaks around 2500  $cm^{-1}$  originated from S–H stretching modes of impurity HDS. On increasing pressure to 10 GPa, the  $\nu_2$  peak became sharp, the  $2\nu_{SD}$  peak split into two peaks, and a combination peak ( $\nu_2 + \nu_L$ ,  $\nu_L$ : lattice vibrational peak) appeared at 1160  $cm^{-1}$ . These spectral changes correspond to an orientational disorder–order phase transition (I–IV) noted in earlier studies.<sup>12,13</sup>

On further compression to 27 GPa, a new shoulder peak appeared at 3585  $cm^{-1}$ , the high-frequency side of the original  $2\nu_{SD}$ . Furthermore, in the region of the bending mode, another peak appeared at 32 GPa at 870  $cm^{-1}$ , 25  $cm^{-1}$  lower than the position of the original  $\nu_2$ . These new peaks gradually grew in intensity as the pressure increased and coexisted with the peaks belonging to phase IV up to 54 GPa. Deuterium substitution

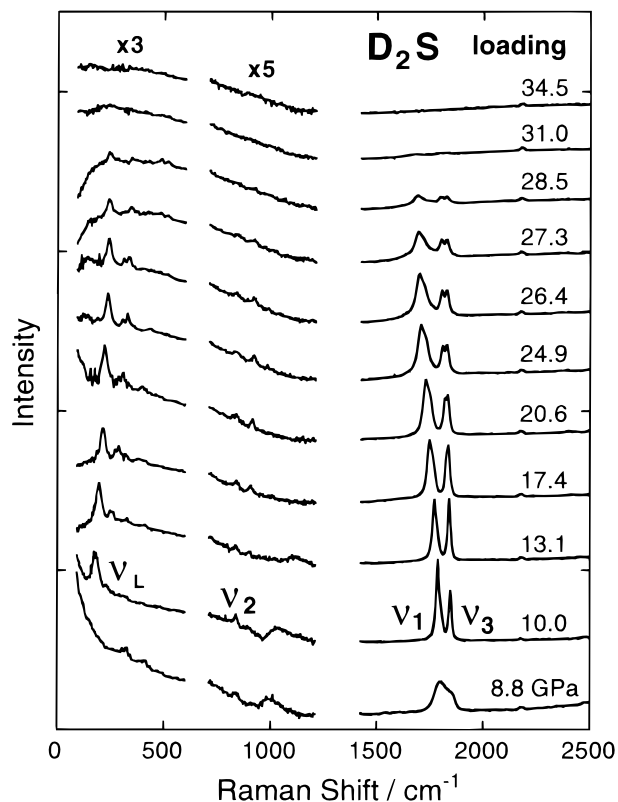


**Figure 2.** Raman spectra of solid  $D_2S$  up to 35 GPa at room temperature.

also reduced the frequency of the new peaks: the peaks of  $D_2S$  are at 847 and 3537  $cm^{-1}$  at 40 GPa, while those of  $H_2S$  are at 1176 and 4768  $cm^{-1}$  at the same pressure. The ratio  $\nu_{H_2S}/\nu_{D_2S}$  was close to  $\sqrt{2}$  (1.39 and 1.35), indicating that these peaks originate from S–D vibration, probably  $\nu_2$  and  $2\nu_{SD}$ .

Figure 2 shows Raman spectra of  $D_2S$  measured up to 35 GPa. The stretching peak split into two narrow peaks,  $\nu_1$  and  $\nu_3$ , and the  $\nu_L$  peak appeared at 10 GPa. These spectral changes also indicate the disorder–order phase transition, consistent with previous work.<sup>12,13</sup> Weak  $\nu_2$  peaks were observed at around 800 and 900  $cm^{-1}$ . On further compression to 27 GPa, two peaks appeared at around 480 and 500  $cm^{-1}$ , as shown in Figure 3. Corresponding peaks were also investigated by Raman scattering from  $H_2S$ ,<sup>9</sup> and the peak positions for  $H_2S$  and  $D_2S$  were almost the same. Hence, these two peaks are assigned not to S–D vibration but to S–S or lattice vibrations. The color of the sample gradually changed from almost transparent to orange, dark red, and black above 27 GPa. Owing to the opaqueness, the incident laser beam could hardly penetrate the sample. Thus, all Raman peaks became weak.

The pressure shifts of the infrared and Raman frequencies are illustrated in Figure 4. The stretching peaks ( $\nu_1$ ,  $\nu_3$ , and  $2\nu_{SD}$ ) slightly shifted to the low-frequency side, and the bending peaks  $\nu_2$  shifted to the high-frequency side with increasing pressure. The pressure behavior of infrared and Raman peaks of  $D_2S$  was similar to that of  $H_2S$ .<sup>12–14</sup> The stretching  $\nu_1$  peak shifted only by  $-5.2$   $cm^{-1} GPa^{-1}$  in phase IV of  $D_2S$ , suggesting that the S–H covalent bonds weaken slightly and the hydrogen bonds become slightly stronger with compression.

As a result of the movement of a gasket hole in the culet, pressure gradients across the sample increased during pressure release. Part of the sample at higher pressure and at lower pressure showed different Raman spectral features. In the part at higher pressure, several signals were detected mainly at 100–

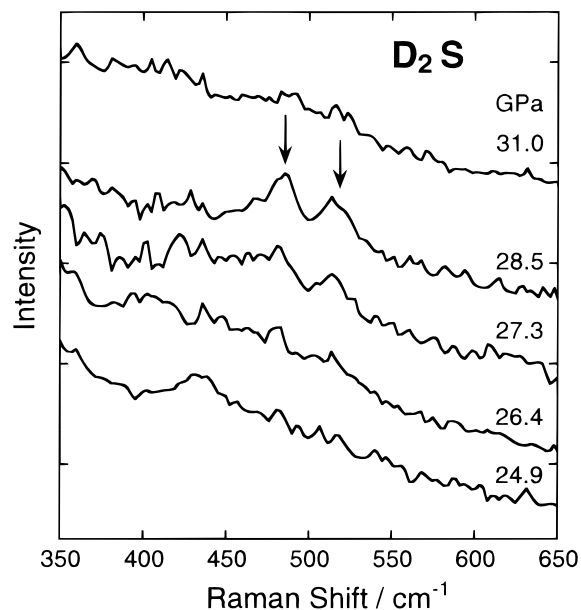


**Figure 3.** Magnification of Raman spectra of solid  $D_2S$  around 27 GPa. The arrows mark the new Raman peaks assigned to S–S stretching modes.

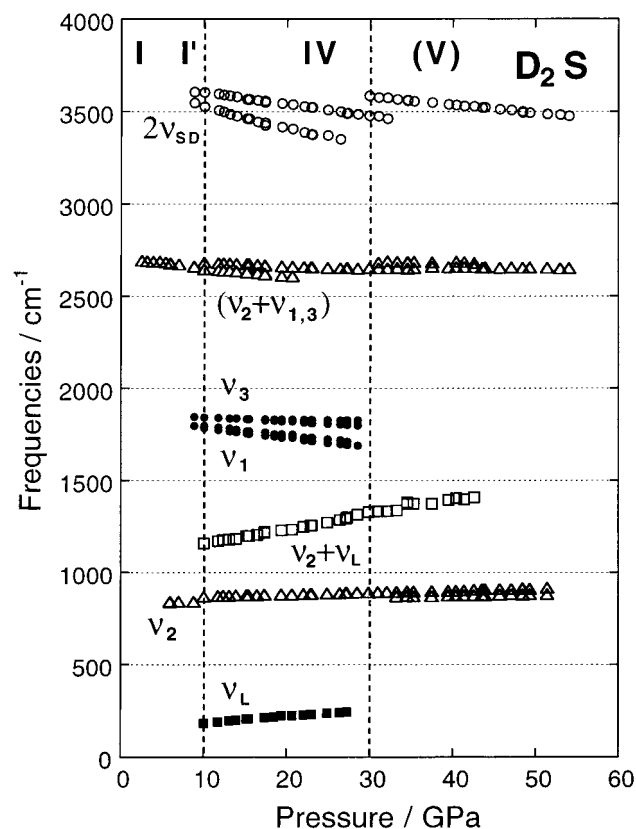


**Figure 4.** Variations in the vibrational frequencies of  $D_2S$  with pressure obtained by infrared (open symbols) and Raman (solid symbols) measurements. Two dashed vertical lines show phase boundaries.

$600\text{ cm}^{-1}$  (Figure 5a) and should be assigned to the S–S stretching modes. Raman spectra observed in the pressure range from 25 to 19 GPa resembled those of the high-pressure low-temperature (hplt) phase of sulfur, which has been reported as a metastable phase obtained above 12 GPa by low-power laser radiation for an ordinary crystalline sulfur.<sup>15</sup> The peak positions of the present sample, 221, 471, and  $506\text{ cm}^{-1}$  at 19 GPa, correspond well to those of the hplt phase, 222, 469, and  $504$

$\text{cm}^{-1}$  at the same pressure. One broad feature observed at  $5.4\text{ GPa}$  at  $100\text{--}600\text{ cm}^{-1}$  was similar to that of helical sulfur.<sup>16</sup> The Raman spectra dramatically changed at around 1 atm: six sharp peaks appeared at  $100\text{--}600\text{ cm}^{-1}$ . All six peaks correspond well to intramolecular vibration of  $S_8$  ring molecule, and the peaks centered at 154, 188, 220, 247, 439, and  $474\text{ cm}^{-1}$  are assigned to  $E_2$ ,  $B_1$ ,  $A_1$ ,  $E_3$ ,  $E_3$ ,  $A_1$  species, respectively.<sup>17</sup>

In the part at lower pressure, Raman peaks were observed at both the S–D and the S–S stretching regions (Figure 5b), indicating that S–D and S–S bonds coexisted in the sample. The peaks observed at  $1600\text{--}1900\text{ cm}^{-1}$  were different from those observed in the loading process: the  $\nu_1$  peak appeared to be much stronger than  $\nu_3$ , and several peaks overlapped with the original  $\nu_1$  and  $\nu_3$  peaks. The additional peak observed at the low-frequency side of  $\nu_1$  could be assigned to the S–D stretching peak of sulfanes (hydrogen polysulfides),  $D_2S_x$ . A broad peak observed at around  $1800\text{ cm}^{-1}$  at  $5\text{--}0.1\text{ GPa}$  was at almost the same position as the peak in phase I, indicating that some  $D_2S$  molecules returned to phase I. Spectral changes at  $100\text{--}600\text{ cm}^{-1}$  region of Figure 5b are similar to those of Figure 5a.

Contrary to the Raman spectra, infrared spectra at the part of the sample at higher pressure (Figure 6a) and at lower pressure (Figure 6b) showed similar patterns in the unloading process. For example, the S–D stretching peaks,  $\nu_1$  and  $\nu_3$ , with almost the same intensity were observed in both parts. This is because transmission infrared spectra reflected S–D bonds persisting inside the sample. A smaller amount of the phase-IV peaks remaining in the part at higher pressure (Figure 6a) only indicates dissociation that proceeded more in the part at higher pressure than at lower pressure. Unreacted  $D_2S$  evaporated when the sample was released to ambient pressure, and some solid remained. The solid showed no detectable peak in the mid-infrared region studied, although sulfur has an infrared peak ( $2\nu_{10}$ ) at  $870\text{ cm}^{-1}$  at ambient pressure.<sup>18</sup>

## Discussion

Infrared absorption and Raman scattering are complementary techniques, and a comparison between vibrational frequencies of  $H_2S$  and those of  $D_2S$  helps to assign every peak of the spectra. In this section, we will interpret the observed infrared and Raman spectra and then demonstrate a model that can consistently explain the molecular dissociation process in  $H_2S$  and  $D_2S$  on the basis of infrared, Raman, and X-ray diffraction data.<sup>19</sup>

Two new infrared peaks observed above 27 GPa (Figure 1) suggest that some S–D bonds are surrounded by molecules in a manner different from phase IV at that and higher pressures. These peaks do not originate from a dissociated phase where the S–D bonds are lost but should be assigned to the fundamental bending and overtone S–D stretching vibrations. The S–D stretching peak usually shifts to lower frequency with increasing pressure, since intermolecular hydrogen bonds become stronger as the molecules approach each other. Thus, the higher position of the new overtone peak than that in phase IV indicates that hydrogen bonds become weak at around 27 GPa. Further, the continuous softening of the overtone vibrations with pressure indicates that the S–D...S hydrogen-bond system still exists above 27 GPa, as in the case of  $H_2S$ .<sup>14</sup> The lower position of the bending peak also indicates weakened intermolecular interaction. Intensity changes in the infrared-absorption peak reflects the change in volume of its related chemical species.

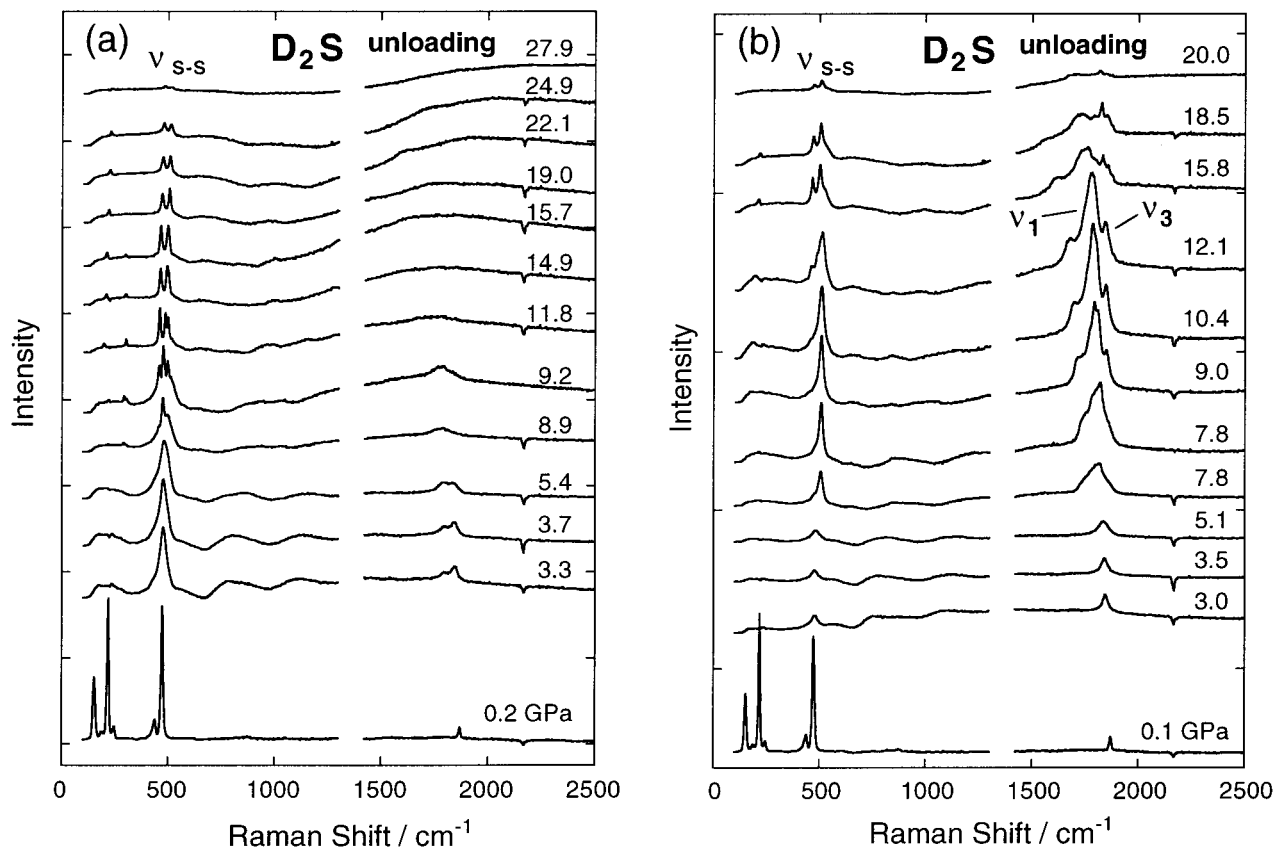


**Figure 5.** Raman spectra of  $D_2S$  measured for the part of the sample at higher pressure (a) and at lower pressure (b) in the unloading process.

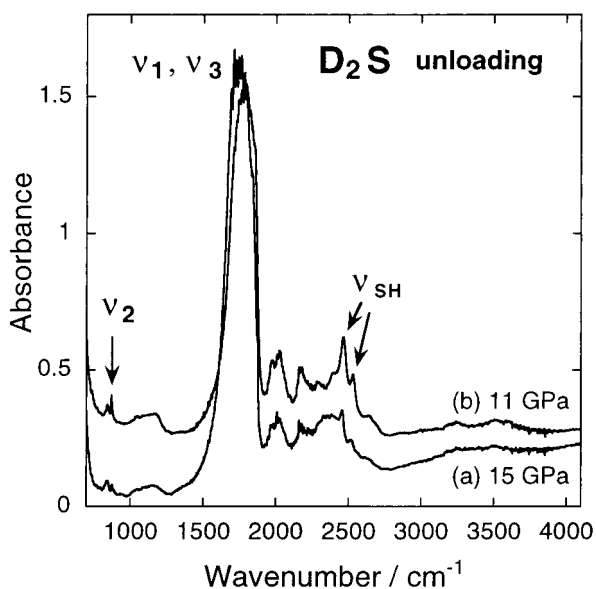


**Figure 6.** Infrared spectra of  $D_2S$  measured for the part of a sample at higher pressure (a) and at lower pressure (b) in the unloading process. The arrows indicate the peaks originating from phase IV.

The intensity of the two new peaks gradually increased with pressure (Figure 1), suggesting a gradual increase of an additional chemical species. The coexistence of the new peaks with the peaks in phase IV up to 54 GPa indicates that additional and original chemical species coexist over a wide pressure range.

On the other hand, several Raman peaks observed in the 100–600  $cm^{-1}$  region suggest that decomposition to sulfur began around 27 GPa. Those peaks probably originate from S–S covalent bonds, indicating formation of sulfur. The occurrence of sulfur also explains the drastic change in lattice vibrational

peaks investigated by Raman experiment on  $H_2S$ .<sup>9</sup> Raman spectral changes observed at 100–600  $cm^{-1}$  during pressure release correspond to the changes in some parts of the sample: the hplI phase of sulfur appeared at 25–19 GPa, helical sulfur around 5 GPa, and then  $S_8$  rings near 1 atm. This interpretation is based on the similarity of the Raman spectra of the present sample and those of sulfur, although Raman spectra of sulfur at high pressures have not been well-defined yet. Helical sulfur was reported to have a chain structure, while the molecular structure of the hplI phase is not clear. The  $S_8$  molecule is a puckered eight-atom ring and is most stable at ambient pressure and temperature. It was reported that the characteristic features of the  $S_8$  ring appear also from high-pressure phases of sulfur when unloading to 1 atm.<sup>15</sup>

Here we consider the process in which  $D_2S$  molecules dissociate under pressure to produce finally  $S_8$  cyclic molecules. The structure of phase IV will yield useful information in explaining the process, since the molecular dissociation occurs around 27 GPa. There is a weak interaction between the nearest sulfur atoms in phase IV in which the molecules form spiral chains along the  $c$ -axis,<sup>3</sup> and the first nearest S–S distance is 3.050 Å at 14.0 GPa, only 0.1 Å longer than the sum of “constant energy radii” of sulfur. Huggins introduced the concept of “constant energy radii” in an equation relating interatomic distances to bond energies.<sup>20</sup> When the interatomic distance is longer than the sum of “constant energy radii”, there is no bonding nature between the atoms. It is natural to imagine that as S–S distances become shorter on further compression, S–S covalent bonds are formed. In addition, the similar transition pressures of  $H_2S$  and  $D_2S$  suggest that the approach of sulfur atoms causes molecular dissociation to form helical sulfur with its chain structure. In the unloading process, the helical sulfur may not revert to  $D_2S$  but change to the  $S_8$  cyclic molecule.



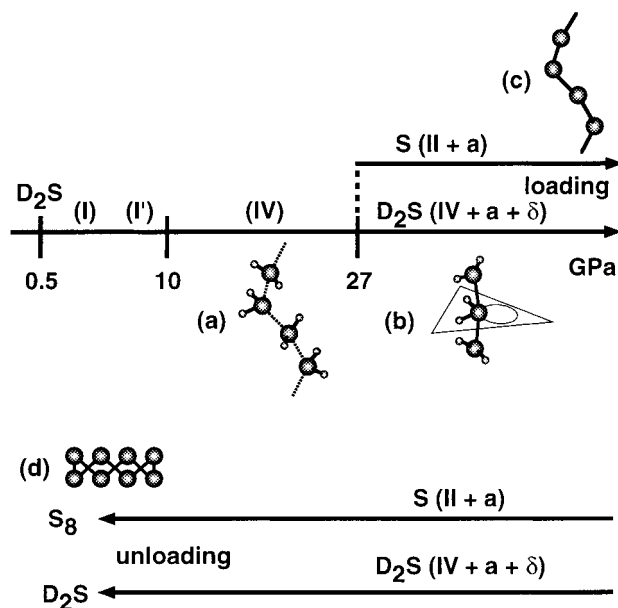


**Figure 7.** Schematic representation for changes in molecular structure and bonding manner of a sample. Part of  $D_2S$  dissociated to form sulfur above 27 GPa (dashed line). Both  $D_2S$  and sulfur persisted in the sample in the unloading process. a: amorphous and  $\delta$ : undefined crystalline phase.

Very recently X-ray diffraction experiments on solid  $H_2S$  were performed up to 50 GPa.<sup>19</sup> The diffraction patterns indicate that several phases exist above 28 GPa, and this is consistent with the infrared and Raman results of the present  $D_2S$  sample. These phases are phase IV of  $H_2S$ , phase II of sulfur, amorphous, and undefined crystalline phase. The amorphous phase can involve both  $H_2S$  and sulfur molecules. No diffraction peaks of the undefined crystalline phase overlapped with peaks of  $\alpha$ -sulfur or  $\beta$ -sulfur. Therefore, infrared peaks observed above 27 GPa will correspond to amorphous or undefined crystalline  $D_2S$ , and Raman peaks will correspond to phase II or amorphous sulfur.

Figure 7 schematically shows likely changes in molecular structure and bonding manner of  $D_2S$  with increasing and decreasing pressure. When  $D_2S$  molecules in phase IV (a) are compressed above 27 GPa, S–S covalent bonds form between the nearest sulfur atoms, resulting in  $(D_2S)_x$  chains (b). Then, deuterium must be removed from  $(D_2S)_x$  chains to produce  $S_x$  chains (c). In the unloading process,  $S_x$  chains will change to  $S_8$  cyclic molecules (d). Sulfur atoms could be tetracoordinated in the  $(D_2S)_x$  chains (b) and bonded to two deuterium and two sulfur atoms such as  $SF_4$ , a trigonal-bipyramidal molecule. The sulfur atoms are assumed to be at apical positions, and two deuterium atoms and one lone pair of electrons at equatorial

positions. This is because the more electronegative ligand prefers to occupy the apical position<sup>21</sup> and the ligand that forms the covalent bond with a central atom such as hydrogen and methyl groups prefers to coordinate in the equatorial position.<sup>22</sup> The apical bonds have shown to be three-center four-electron bonds in a trigonal-bipyramidal molecule. When the  $(D_2S)_x$  chains are formed, the deuterium atoms move from hydrogen-bond axes, resulting in the weakening of hydrogen bonds. Thus, the  $(D_2S)_x$  chains (b) will explain the infrared peaks observed above 27 GPa. On the other hand, the observed Raman peaks can be explained as S–S stretching peaks of  $S_x$  and as S–D stretching peaks of remaining  $D_2S$ .

The present results revealed that the molecular dissociation of  $D_2S$  occurred around 27 GPa, that the dissociation caused formation of sulfur, and that several kinds of S–D or S–S bonds coexisted when the sample was compressed to 27 GPa. Pressure-induced sulfur formation may offer the prospect of reconstruction of chemical bonds under high pressure.

## References and Notes

- (1) El Saffar, Z. M.; Schultz, P. *J. Chem. Phys.* **1972**, *56*, 2524.
- (2) Endo, S.; Ichimiya, N.; Koto, K.; Sasaki, S.; Shimizu, H. *Phys. Rev. B* **1994**, *50*, 5865.
- (3) Fujihisa, H.; Yamawaki, H.; Sakashita, M.; Aoki, K.; Sasaki, S.; Shimizu, H. *Phys. Rev. B* **1998**, *57*, 2651.
- (4) Endo, S.; Honda, A.; Sasaki, S.; Shimizu, H.; Shimomura, O.; Kikegawa, T. *Phys. Rev. B* **1996**, *54*, R717.
- (5) Hemley, R. J.; Jephcoat, A. P.; Mao, H. K.; Zha, C. S.; Finger, L. W.; Cox, D. E. *Nature* **1987**, *330*, 737.
- (6) Sakashita, M.; Yamawaki, H.; Fujihisa, H.; Aoki, K.; Sasaki, S.; Shimizu, H. *Phys. Rev. Lett.* **1997**, *79*, 1082.
- (7) Goncharov, A. F.; Struzhkin, V. V.; Somayazulu, M. S.; Hemley, R. J.; Mao, H. K. *Science* **1996**, *273*, 218.
- (8) Aoki, K.; Yamawaki, H.; Sakashita, M.; Fujihisa, H. *Phys. Rev. B* **1996**, *54*, 15673.
- (9) Yamagishi, M.; Furuta, H.; Endo, S.; Kobayashi, M. *Science and Technology of High Pressure*, in press.
- (10) Pruzan, Ph.; Wolanin, E.; Gauthier, M.; Chervin, J. C.; Canny, B.; Häusermann, D.; Hanfland, M. *J. Phys. Chem. B* **1997**, *101*, 6230.
- (11) Mao, H. K.; Xu, J.; Bell, P. M. *J. Geophys. Res.* **1986**, *91*, 4673.
- (12) Shimizu, H.; Nakamichi, Y.; Sasaki, S. *J. Chem. Phys.* **1991**, *95*, 2036.
- (13) Shimizu, H.; Murashima, H.; Sasaki, S. *J. Chem. Phys.* **1992**, *97*, 7137.
- (14) Shimizu, H.; Ushida, T.; Sasaki, S.; Sakashita, M.; Yamawaki, H.; Aoki, K. *Phys. Rev. B* **1997**, *55*, 5538.
- (15) Häfner, W.; Olijnyk, H.; Wokaun, A. *High-Pressure Res.* **1990**, *3*, 248.
- (16) Eckert, B.; Jodl, H. J.; Albert, H. O.; Foggi, P. *Frontiers of High-Pressure Research*; Plenum Press: New York, 1991; p 143.
- (17) Scott, D. W.; McCullough, J. P.; Kruse, F. H. *J. Mol. Spectrosc.* **1964**, *13*, 313.
- (18) Anderson, A.; Smith, W.; Wheelton, J. F. *Chem. Phys. Lett.* **1996**, *263*, 133.
- (19) Fujihisa, H.; et al. Manuscript under preparation.
- (20) Huggins, M. L. *J. Am. Chem. Soc.* **1953**, *75*, 4126.
- (21) Deiters, J. A.; Holmes, R. R.; Holmes, J. M. *J. Am. Chem. Soc.* **1988**, *110*, 7672.
- (22) Wasada, H.; Hirao, K. *J. Am. Chem. Soc.* **1992**, *114*, 16.